Civil Engineering and Architecture 11(6): 3260-3277, 2023 http://www.hrpub.org
DOI: 10.13189/cea.2023.110602

Using Sustainble Architectural Wind-Driven Tubes Roof-Pond to Save Energy on Roof Cooling Loads in Tropical Climate: CFD Modeling and Experimental Investigations

Danny Santoso Mintorogo

Department of Architecture, Petra Christian University, Indonesia

Received January 17, 2023; Revised July 8, 2023; Accepted August 15, 2023

Cite This Paper in the Following Citation Styles

(a): *[1] Danny Santoso Mintorogo , "Using Sustainble Architectural Wind-Driven Tubes Roof-Pond to Save Energy on Roof Cooling Loads in Tropical Climate: CFD Modeling and Experimental Investigations," Civil Engineering and Architecture, Vol. 11, No. 6, pp. 3260 - 3277, 2023. DOI: 10.13189/cea.2023.110602.*

(b): *Danny Santoso Mintorogo (2023). Using Sustainble Architectural Wind-Driven Tubes Roof-Pond to Save Energy on Roof Cooling Loads in Tropical Climate: CFD Modeling and Experimental Investigations. Civil Engineering and Architecture, 11(6), 3260 - 3277. DOI: 10.13189/cea.2023.110602.*

Copyright©2023 by authors, all rights reserved. Authors agree that this article remains permanently open access under the terms of the Creative Commons Attribution License 4.0 International License

Abstract The global increase in energy-related crises has led to the development of innovation to save energy resources for passive cooling or heating to cope with convective roof-pond as conventional one which uses open-close layers. Therefore, this research was conducted to save cooling energy by enhancing the conventional roof-pond through the implementation of a new application in the form of a wind-driven tube roof-pond. Several considerations: First, this roof pond is classified as an open roof pond equipped with a V-shaped shading device to block solar radiation from the sun in the morning and afternoon utilizing gusts of wind to cool the water temperature in the roof pond. Second, eliminating the traditional roof pond which operates mechanically open–close the layer water pond during the day if the roof pond is closed during the day when solar radiation is hot, the water temperature will increase because there is no cross ventilation or wind blowing to cool the water roof pond in tropical hot and humid climates. Third: energy saving of cooling loads from building will include building skin loads, windows cooling loads and roof cooling loads. The roof pond will reduce heat flux most of all cooling loads from the roofs. So the roof pond research with the implementation of iron tubes accelerates cooling due to a lot of wind gusts so that it can save cooling load energy from the heat loads of the roof. The process methodology involved simulating the transportation of forced wind through a series of iron tubes using CFD. The convective cooling of ponds was also enhanced to examine the V shading devices at right angles. Moreover, the experimental models were used to determine the water pond and room ambient temperatures using Onset Hobo data loggers type U12 equipment and the final result showed that cooler of water pond occurred at 0.2 to 1℃ which is crucial among of temperatures in tropical climate zone and obtaining room ambient temperature of 0.2 to 0.7℃ in a wind-driven tubes system. It was concluded that the wind-driven roof-pond has a cooling load saving of 100 – 250 Watts per square meter day and night with wind-driven tubes.

Keywords Sustainable, Architectural Wind-Driven Tubes, Roof-Pond, Saving Energy, Roof Cooling Load, Tropical Climate

1. Introduction

The cooling of flat rooftops requires the adoption of several strategic systems such as instant cool roofs, layering of bitumen, ventilated double flat rooftops, as well as an evaporative and common cooling rooftop with water

known as a roof-pond. The working principle of a conventional roof-pond involves providing shade, which is usually opened at night, over the water pond. These open-closed shading devices can be operated manually and automatically, and the water used as the cooling medium remain is usually cool, natural, and eco-friendly. Moreover, convection passive cooling is defined as a natural process involving the movement of air molecules in line with temperature changes. It was stated by G. Carrilho [1, 2] that ventilated, evaporative, radioactive, and skytherm night convection roof-pond are examples of passive cooling strategies in buildings. Table 1 further shows a roof-pond with night sky radiation (skytherm) and wind convective cooling (day-night).

A study proposed an enhanced roof-pond which involves using wind speed to generate convection cooling with submerged iron tubes and V shape shading devices in East Java, city of Surabaya – Indonesia during the warm, humid, and tropical climate. The latitude and longitude of the area are 7,25°S and 112,47°E, respectively, and the area was also observed to be close to the equator, thereby, causing the fluctuation of the sky's irradiance. The average horizontal irradiance recorded annually within five years from 2017 to 2021 was found to be 146, 160, 163, 156, and 150 kWh/m^2/year, respectively, and 4.8, 5.3, 5.4, 5.1, and 4.9 kWh/m^2/month correspondingly [3]. Moreover, the rooftops, walls, windows, and doors received horizontal solar radiation of 35%, 18%, and 16%, respectively [4]. Several types of enhanced roof-ponds have been developed effectively to diminish the conversion of heat in order to trigger more energy consumption [5]. This is necessary because most buildings utilize enormous global energy which was estimated at 35 to 40% and also found to be contributing 35% to the world's overall GHG production [6, 7].

The other factors influencing the cooling of roof-ponds include mean temperature and wind speed as shown in Figure 1. It was discovered that the maximum outdoor temperature recorded for the complete year was from August to November with 33, 35, 35, and 34°C respectively [8]. The highest mean daily temperature was found to be around September and October because the sun's position was adjacent to the equator while the lowest was 21°C during the day and 19°C at night from August to October. Moreover, the high wind mostly occurred at the meantime during the dry seasons from May to October with a speed of 2.8, 3.3, 3.3, 3.6, 3.3, and 2.8 m/s, respectively, and the maximum was recorded to be 5.3 m/s between August and September. According to the weather Atlas [9], August is usually the windiest month in Surabaya with an average speed of 2.75 m/s while the calmest is April with the lowest average speed of 1.75 m/s. It was also observed that the humidity interval in Surabaya 2021 was normally 68% to 83% with the most humid months found to be January – May while the least was recorded from August – November [9].

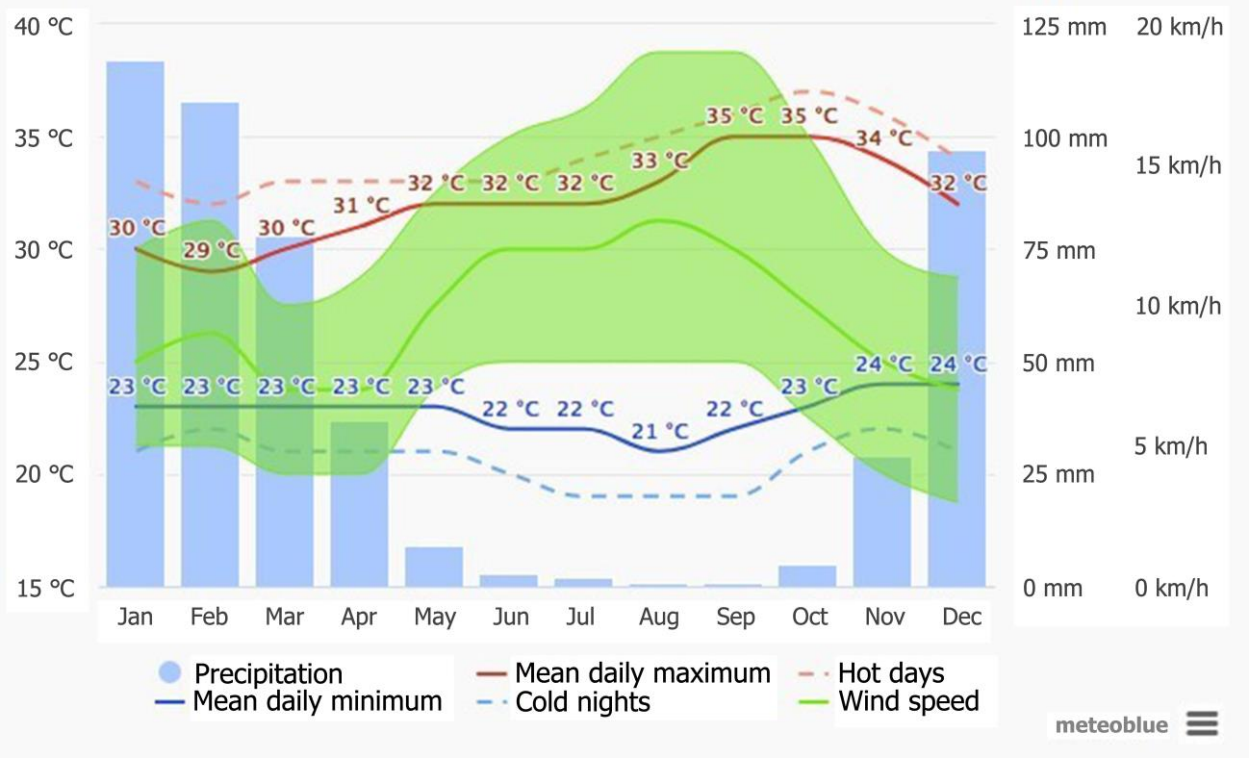

Figure 1. Max. and Min. temperature, wind speed annually (Source: NASA, 2022) [3]

Table 1. Sorted variant of roof-ponds with evaporative and convective cooling

Roofpond Types	Perform	Energy Saves	References
Uncovered pond with /without spray water	10 - 50 cm water depth	*Reduced heat flux 55% *Thermal fluctuated bare roof to roof-pond 1.6 - 3℃	[10, 11]
Ventilated Roof-pond	9-10 cm water depth. Fixed insulated layer above ventilated gap.	Thermal fluctuated bare roof to r-pond 1.6 - 3℃	[12, 13, 14, 15, 16, 17]
	30 cm gap water & insulated layer	Cooler 3℃ than mean temperature	
	Fan assisted cooling	Reduced indoor temp to max 7℃	
Open roof pond	Min 30 cm water depth	Reduced 5.6℃ in warm climate	[18]
Pond without spraying water	Better performance & consume slightly water on pool	Reached indoor temp. to 33.3 – 35.3℃	[19]

1.1. Hypothesis

The aim of double cooling strategies is to enhance the water roof-pond using wind-driven and immersed iron tubes that work for 24h including daytime and nighttime. The operation involves blowing cold wind through the iron tubes through the process known as conduction and convection to speed up the cooling effects. Furthermore, the V shape shading devices installed on the roof-pond have a Venturi effect which was intended to enhance the cooling of water elements during the day and at night.

1.2. Aim of the Research

This research aims to design an appropriate open roof-pond with unmechanical shading devices to open and close the pond layers as well as to fasten the cooling water pond and save the cooling load's energy daily using wind-driven tubes.

2. Materials and Methods

2.1. Prototype Models

There are three prototype models comprising additional iron tubes and a V-shading roof-pond to monitor the effect of airflow behavior on heat transfer. The first, second, and third models were conventional concrete rooftop, common roof-pond, and the wind-driven type, respectively, and the ANSYS Fluent simulator which is a replication of computational fluid dynamic (CFD) software was applied. Moreover, CFD analysis was used due to the convective and conductive cooling aspects of wind-driven roof-pond. The process involved examining the wind flow behavior with a focus on its average speed, pattern, and characteristic before and after entering the iron tubes and appropriate values were obtained from the local weather station. Certain aspects of the shading devices installed on top of wind-driven roof-pond to enhance convective cooling were also investigated, and these include:

a. The opening angles of shading devices at 0º, 10º, 15º, 30º and 45º
b. The lower space of V shape to the water pond
c. Addition of a wind vane to guide the flow pattern

An experimental model was also applied, hence the three models were first tested simultaneously using one room as a conventional roof-pond realm. The second aspect focused on an enhanced wind-driven type submerged with iron tubes and the third is a conventional flat concrete roof.

2.2. Wind-Driven Iron Tubes Roof-Pond

The purpose of wind-driven iron tubes is to enhance the conventional roof-pond based on the theory of convective cooling (Figure 2a) which aims to further cool immeasurably water elements at a depth of 25 cm in the pond and series of immersed iron tubes (Figure 2b,c,d).

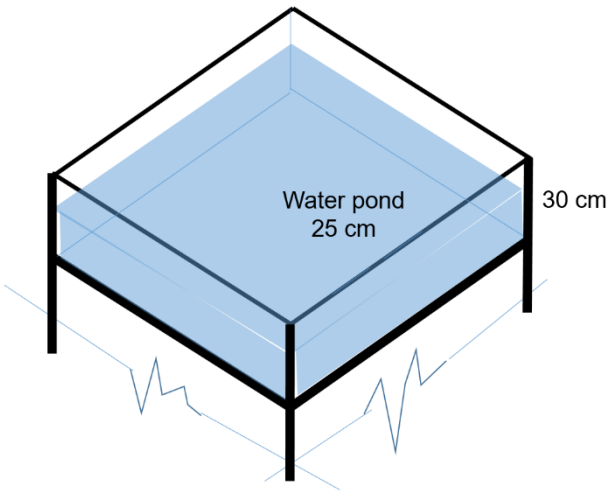

(a)

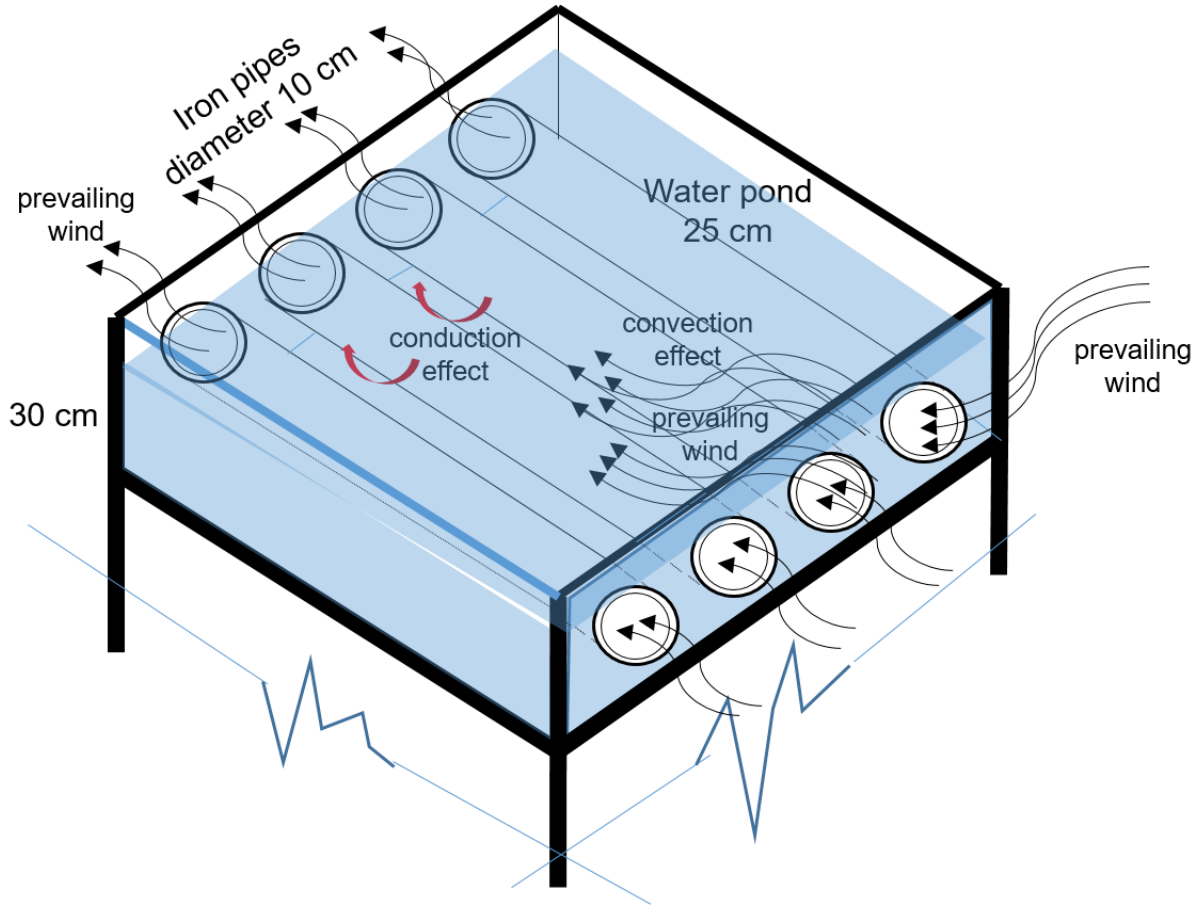

(b)

(c) (d)

Figure 2. (a) Conventional roof-pond, (b) Wind-driven roof-pond with submerged iron tubes to enhance cooling (c, d) Under constructed iron tubes roof-pond model.

2.3. Construction Materials Used to Test the Models

The three experimental models were placed simultaneously to obtain concrete rooftop surface temperature, water elements roof-pond temperatures, test-room indoor temperatures, and shaded outdoor temperatures. The test was conducted on the rooftop of Petra Christian University in Surabaya during the dry seasons of the humid tropical climate which was from June to November. The models were designed using similar materials and sizes with a dimension of 1 m x 1 m x 1 m and a height of 0.3 m as indicated in Figure 3. Each model was mounted at a 0.5 m distance from the rooftop surface. They were all constructed with thermal insulation to prevent solar radiation from overheating the four facades. The insulation layers are stated as follows:

a. Styrofoam 20 mm (interior).
b. Kalsi board 4 mm (facades).
c. Aluminium foil 1 mm (facades).
d. Air space 10 mm (cavity walls-facades).
e. Kalsi board 4 mm (facades).

The main structures were built with an iron L profile and welded at the joints while the shading plates were mostly aluminum sheets.

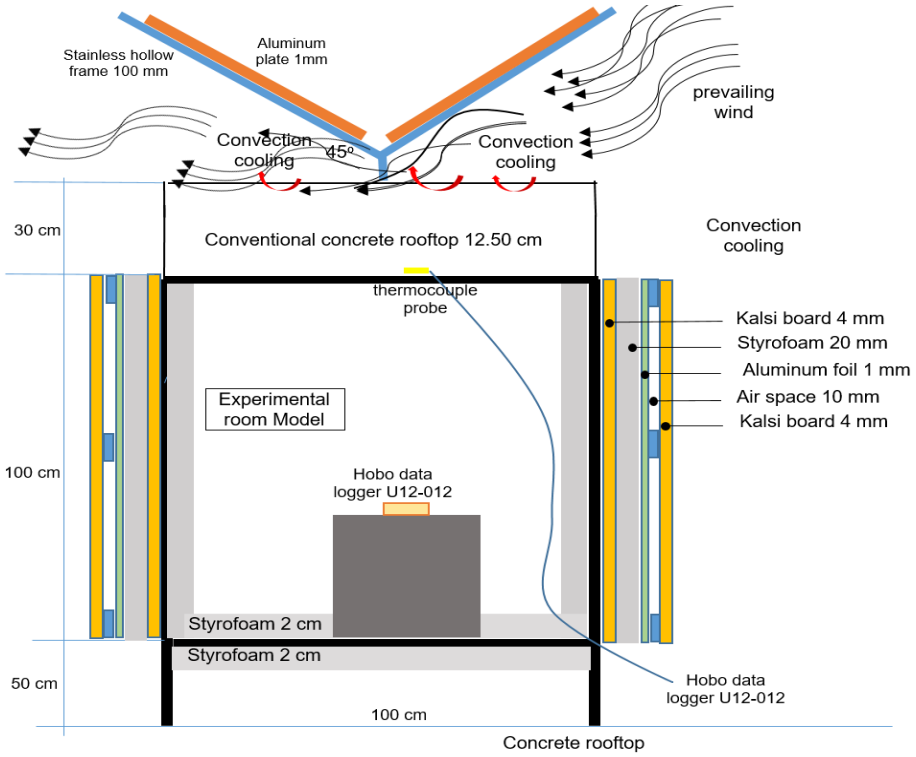

(a)

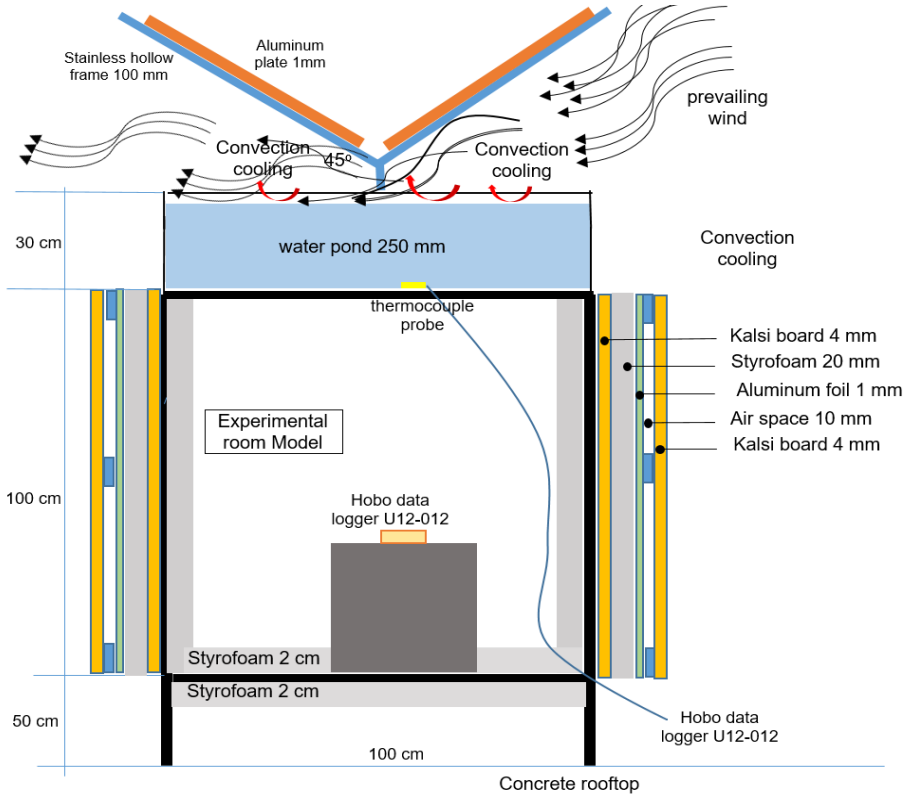

(b)

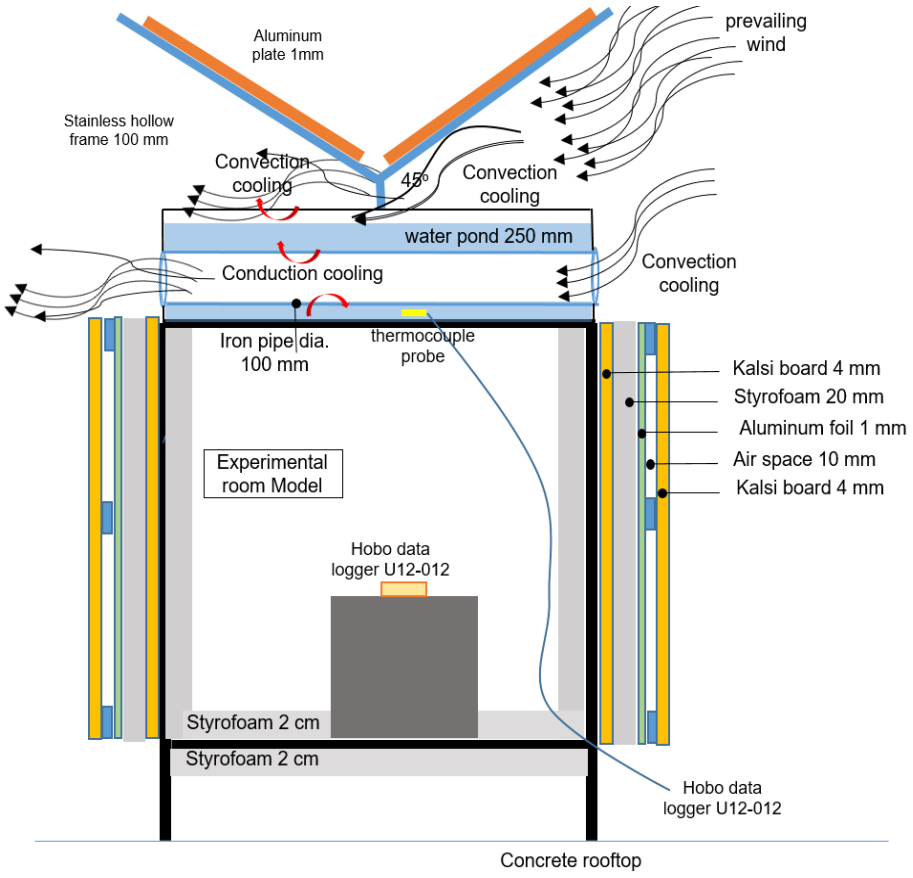

(c)

Figure 3. (a) Conventional concrete rooftop with V shading device, (b) Conventional roof-pond with V shading device, and (c) Wind-driven roof-pond with submerged iron tubes and V shape shading devices.

2.4. The Experimental Tools

The experiment was conducted to determine all relevant temperatures except relative humidity and solar radiation. The aspects tested include:

a. Concrete surface and tested indoor room temperatures.
b. Conventional roof-pond of the water element and established indoor room temperatures.
c. Wind-driven water element roof-pond and experienced indoor room temperatures.
d. Shaded outdoor temperature (day and night).

The Onset HOBO data loggers were used to monitor the thermal performances. The six-unit of Onset Hobo data loggers U12 temperature, relative humidity, light, or external data logger presented in Figure 4a was applied to determine thermal fluctuations due to its high accuracy in measuring temperature levels. Moreover, air/water/soil temperature sensor probes in Figure 4b were used to determine the surface and water temperatures in the wind-driven roof-pond project.

(a) (b)

Figure 4. (a) Onset Hobo Data Logger U12-012 with 1 external port; (b) Sensor temperature probes

Onset Hobo data loggers U12-012 specifications:

Temperature:

a. Capacity monitoring range (- 20º to 70℃).
b. Accuracy range: ± 0.35℃ from 0℃ to 50℃

Relative Humidity:

a. 5% to 95% RH
b. Accuracy range: ± 2.5% typical, 3.5% maximum, from 0 to 90%

Sensor Probe TCM6-HD:

a. Measurement range: -40º to 100℃
b. Accuracy: response time in the air: 2 min.
c. Accuracy: response time in stirred water: 30 sec. typical to 90%

2.5. The V Appearance Shading Devices

The shading devices and all tested models were used based on certain considerations and several pieces of evidence stated as follows:

a. The installation of shading plates closely on top of the roof-pond increases the water-pond temperature to approximately 35℃ during the daytime in hot and humid tropical climates due to high-intensity solar radiation of 792 $W.m^{-2}$ on horizontal surfaces [20].
b. The effect of convective cooling wind-driven over water surface pond by V-shaped shading plates installed on top of roof-pond and conventional flat rooftop is as shown in Figure 3 (a, b, c).
c. The construction of V-shaped shading plates with 60 cm length each from the center obstructs the shortwave of the sun ray and bounces back the longwave.

2.6. The V Appearance Shading Devices Simulation

ANSYS was used to simulate the successful flow pattern in iron tubes and to fasten wind speed. The wind streaming through the shading plates was also evaluated to obtain the right angles in order to determine the effective impact of convective cooling.

The parameters set on the ANSYS based on the yearly average in Surabaya are stated as follows:

a. Wind speed: 2.31 m/s.
b. The density of air: 1.225 kg/m^3
c. Length of the cube (L): 1 m
d. Diameter of the cube (D): 0.1 m

The zero-degree shading plate does not have lamina wind flowing through the shading gap but turbulence wind flowed through the tubes at a speed estimated to be 0.738 – 1.477 m/s as indicated in Figure 5a. It was discovered from the other patterns at 15º and 30º that little wind passed over the surface of the water pond with the laminar flow observed on the shading plate while the turbulence flow was through tubes at 1.399 m/s as presented in Figures 5b and c. Meanwhile, the shading plate with an angle of 45 degrees was discovered to be successful at causing the laminar wind to blow against the surface of the water pond while the turbulence flow was experienced in the iron tube as indicated in Figure 5d.

The airflow across the shading was found to be external with ReL=1,581.105 and laminar while the flow in iron tubes with ReD=1,581.104 was turbulent. The simulation equations on CFD on laminar flow were final without any validation process but the turbulence flow aspect is a hot issue considering the application of the viscous flow equation according to the shape of the meshing and flow characteristics

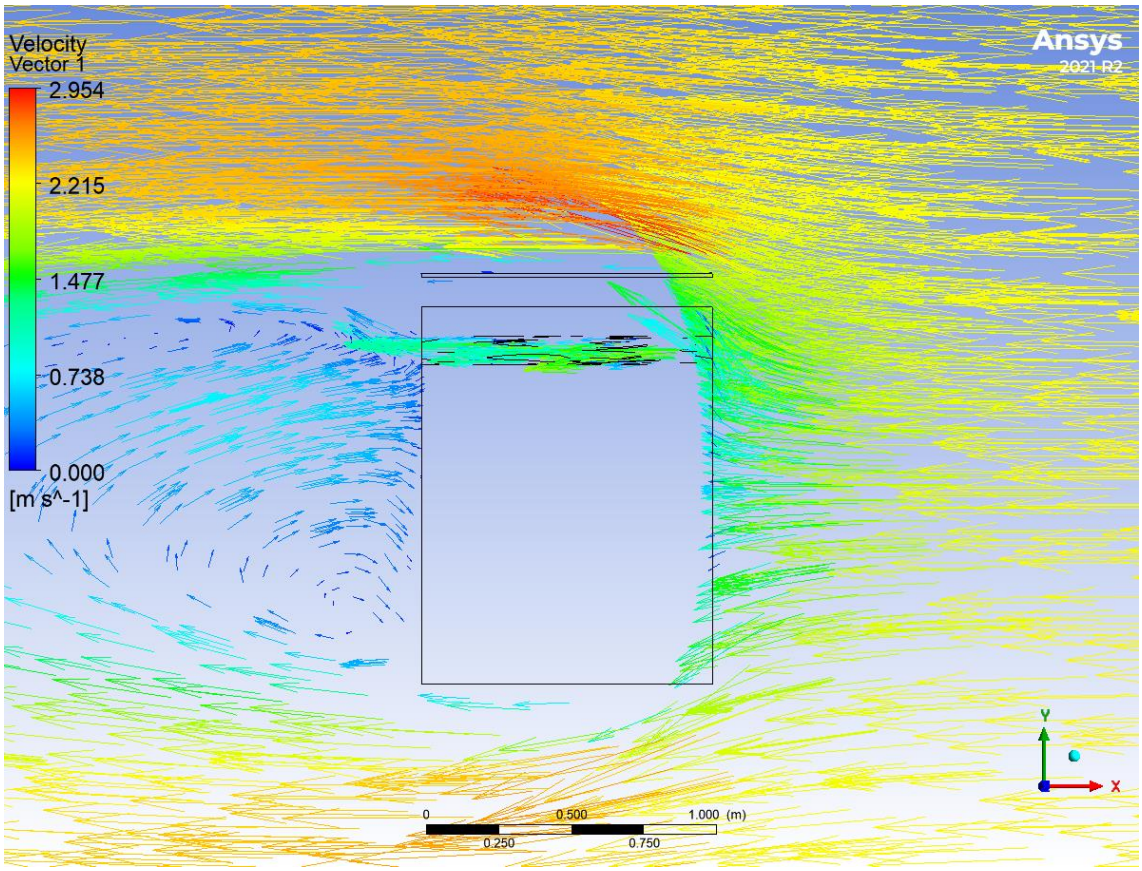
Velocity
Vector 1
2.954
2.215
1.477
0.738
0.000
[m s^-1]
Ansys
2021 R2
Y
X
0
0.500
1.000 (m)
0.250
0.750

(a)

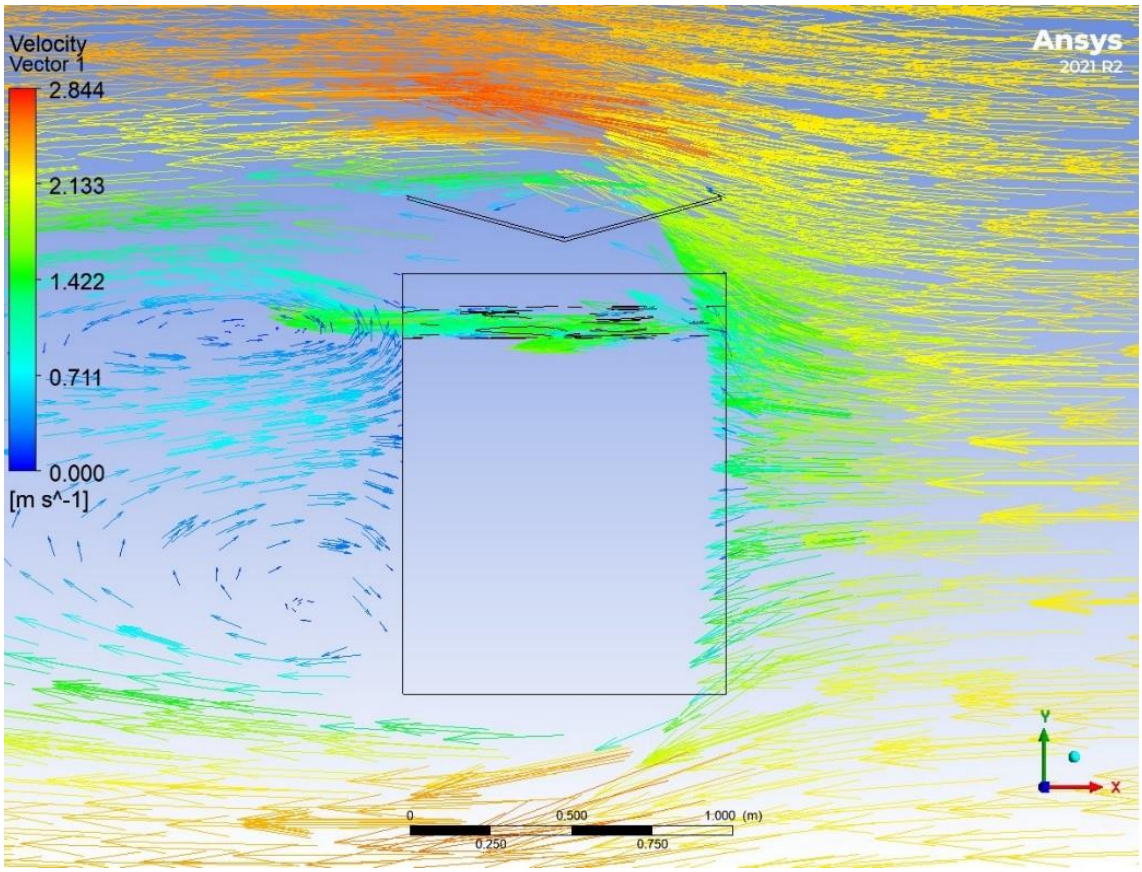
Velocity
Vector 1
2.844
2.133
1.422
0.711
0.000
[m s^-1]
Ansys
2021 R2
Y
X
0
0.500
1.000 (m)
0.250
0.750

(b)

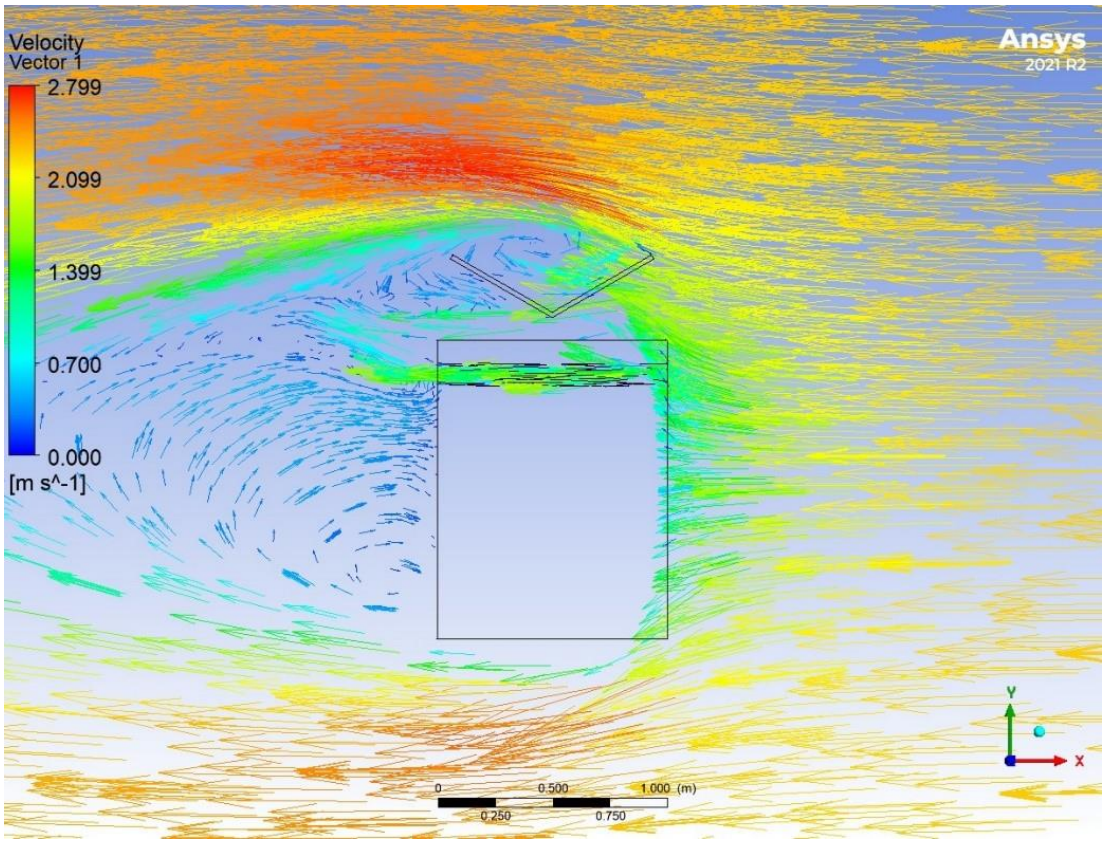

(c)

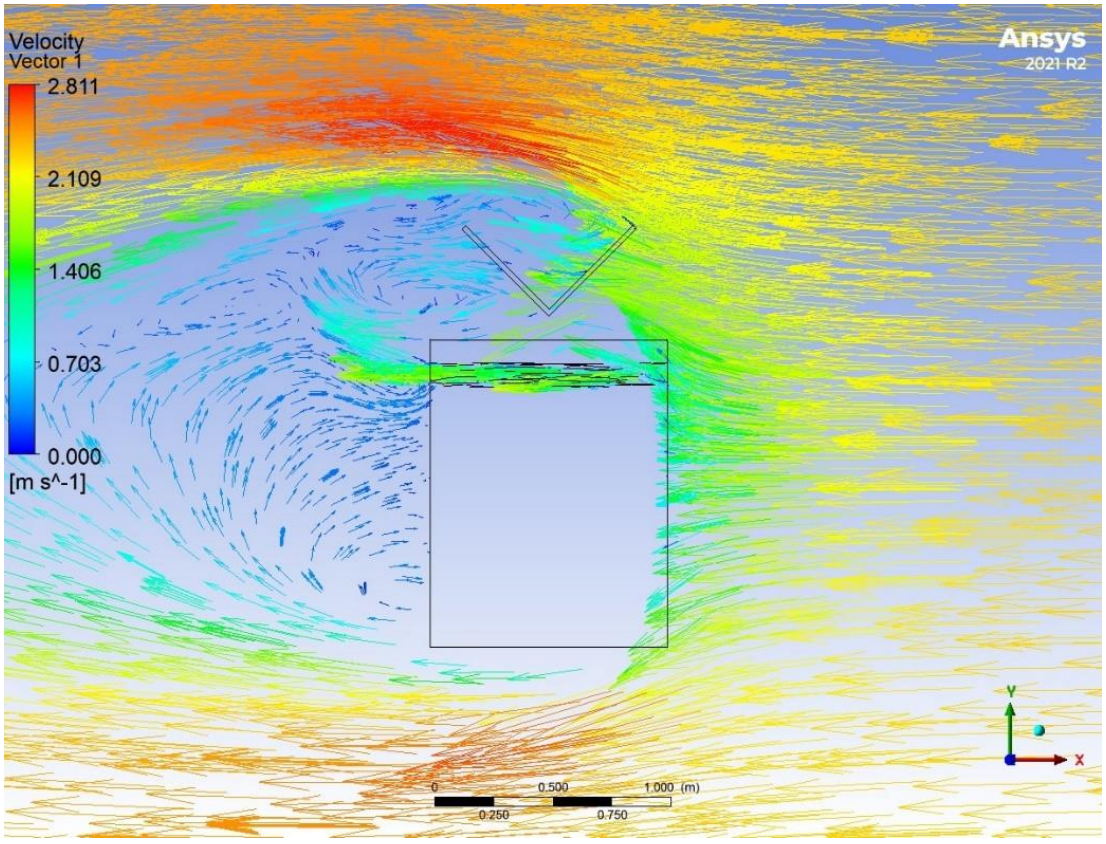

(d)

Figure 5. (a) Wind flow pattern in the iron tube and shading plate 0º, (b) wind pattern in the iron tube and shading angle 15º, (c) wind pattern in the iron tube and shading angle 30º, (d) wind pattern in iron tube angle 45º

3. Results and Discussion

3.1. Shading Device Angles

V shading plates as shown in Figure 5 are presented as follows:

a. V form shading plate was positioned horizontally within 10 cm from the roof-pond but was unable to cause the wind to blow through the gap and trigger convective cooling in the water roof-pond as shown in Figure 5a.
b. At angle 15º, the V-shaped shading plates failed to direct the wind through the water level roof-pond as shown in Figure 5b.
c. At angle 30º, the air blasted slightly appeals to the gap between the roof-pond and the shading due to the back wind suction of V shading as shown in Figure 5c.
d. At angle 45º, the wind gusts tended to pass through the bottom of V shading and surface of water elements to ensure it often comes into contact with the roof-pond, thereby, leading to the frequent occurrence of a convective cooling effect as shown in Figures 5d and 6b.
e. Laminar wind flow ReL = 1,581.105 as indicated in Figure 6b.

3.2. Wind-Driven Iron Tubes

The simulation of wind-driven tubes on the roof-pond allows the successful passage of wind with the speed observed to have slightly increased after entering the tube. This consequently led to the occurrence of convective cooling on iron-tube surfaces as shown in Figure 7a with a turbulent flow (ReD=1,581,104).

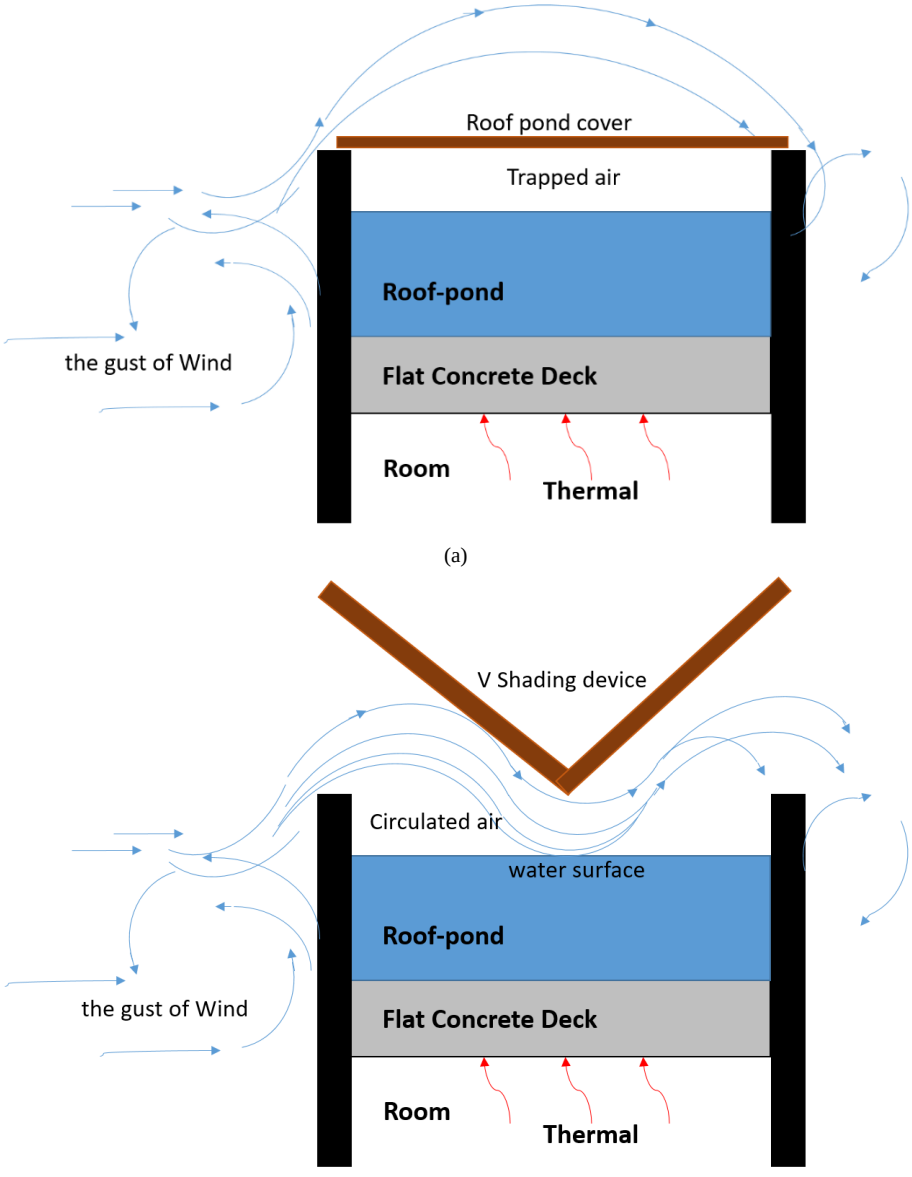

Figure 6. (a) Wind breezes pattern over common roof-pond (b) Laminar wind breezes behavior with V shape shading devices.

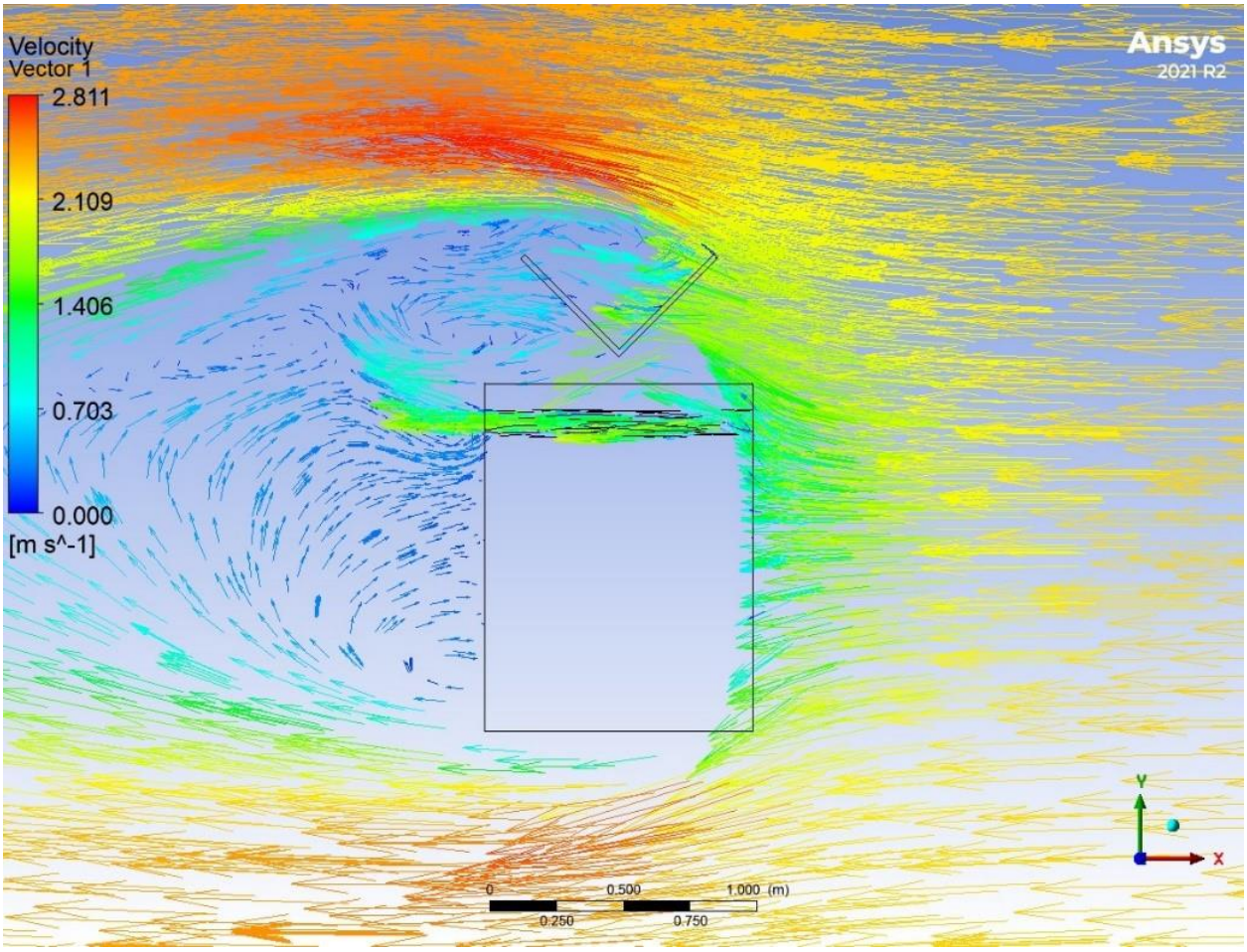

(a)

(b)

Figure 7. (a) ANSYS simulator showing wind breezes pattern on the iron tube, (b) experimental wind-driven iron tubes model on site

3.3. Experimental Models of Thermal Performances with Shading V Shape

3.3.1. Hourly & Yearly Average Thermal Performance of Water Roof-Pond

The sun's position is usually close to the equator from March to September every year and this triggers solar radiation which subsequently increases thermal energy. It is important to note that the temperature is mostly quite low during the rainy season in March compared to September when it is normally extremely hot and dry. Meanwhile, the sun is usually far from the equator at 27.5 degrees North and South from June to December.

In conventional and wind-driven conditions, water pond temperatures were found to be 25° to 27℃ at night and approximately 26 to 29℃ during the day in March as indicated in Figure 8a. Meanwhile, a severe increase was recorded in September with relatively 5℃ in the daytime and 3℃ at night as presented in Figure 8b.

The minimum temperature of 26℃ was recorded in roof-pond water at 8 am during the rainy season in March while the maximum in the conventional type was 29℃. However, it was discovered that the wind-driven pond water temperature was 29.4℃ at 4 pm while the outdoor air temperature was 29.6℃ which was hotter than the water molecule as presented in Figure 8a.

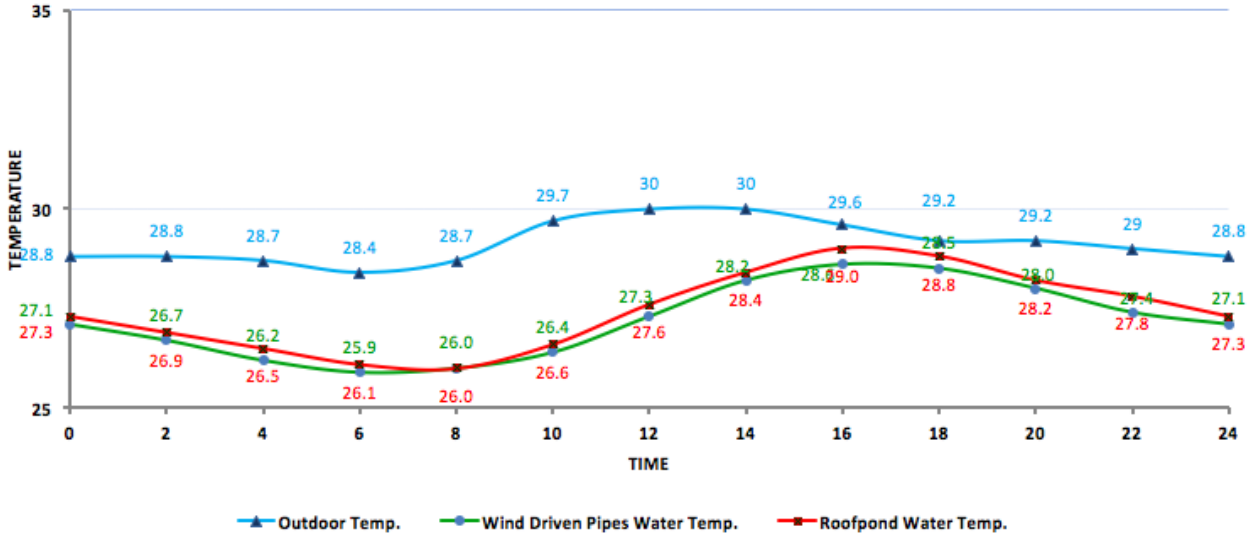

(a)

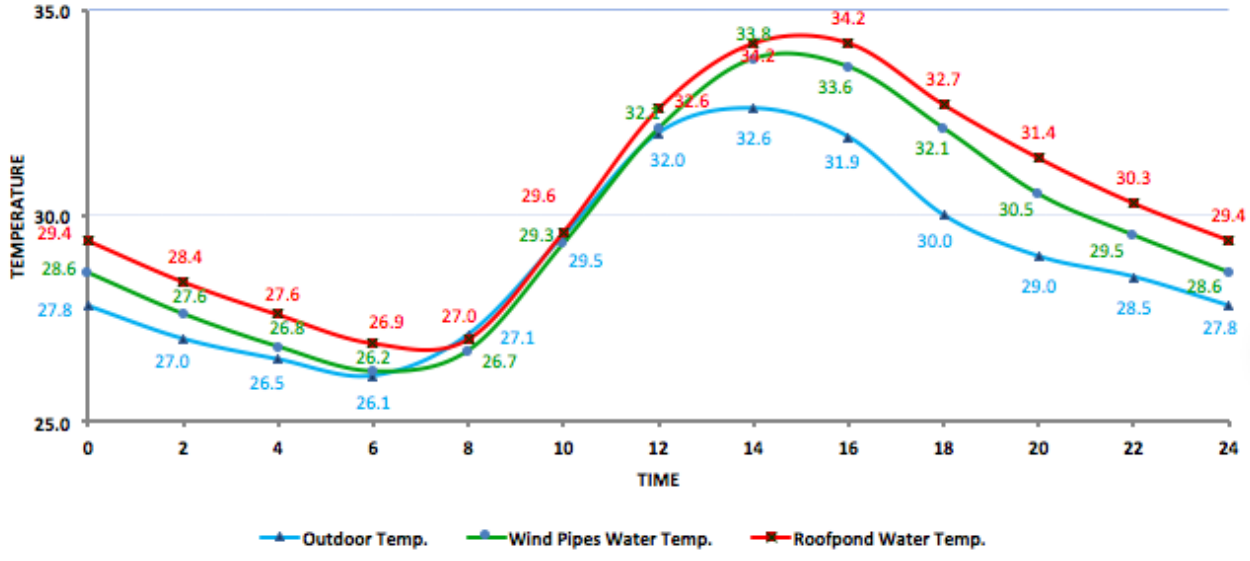

(b)

Figure 8. (a) Hourly Water Molecule Temperature in March 2021, (b) Hourly Water Molecule Temperature in September 2021

The atmosphere was extremely hot in September and the minimum ambient temperature recorded at 6 am was 26.1℃ while the regular water pond had 26.9℃. The water pond's wind-driven temperature was observed to be closer to the value for the outdoor which was relatively 26.2℃. Moreover, the maximum water temperature recorded at 4 pm rather than noon was 34.2℃, 33.6℃, and 31.9℃ for common water roof-pond, wind-driven, and shaded outdoor respectively as shown in Figure 8b.

Figures 8a and b further indicated that the hourly average water molecule temperatures of wind-driven roof-pond were always cooler at approximately 0.2 to 1℃ than the common types during the critical months of March and September. This phenomenon is believed to be caused by the whooshing air through iron tubes based on a convective and conductive cooling process that lasted for 24 hours.

Figure 9a shows the mean daytime yearly water molecules temperatures during the critical months of March, June, September, and December, and those related to the wind-driven pond were all found to be cooler at 0.3 – 0.4℃ than the common type except in June when it was higher by 0.2℃ in daytime and nighttime. Moreover, the phenomenal cool wind-driven water temperatures of 0.5 to 1℃ were recorded in March, September, and December 2021 at nighttime except in June as indicated in Figure 9b.

3.3.2. Hourly & Yearly Average Thermal Performance for Tested Room Roof-Pond

The water temperatures of the tested room roof-pond were found to be always cooler, at approximately 0.2º to 1℃, than the common type recorded during the critical months of March, September, and December, except June in accordance with the wind-driven roof-pond. This phenomenon was caused by the whooshing air through iron tubes which ensured 24-hourly convective and conductive cooling as presented in Figure 9.

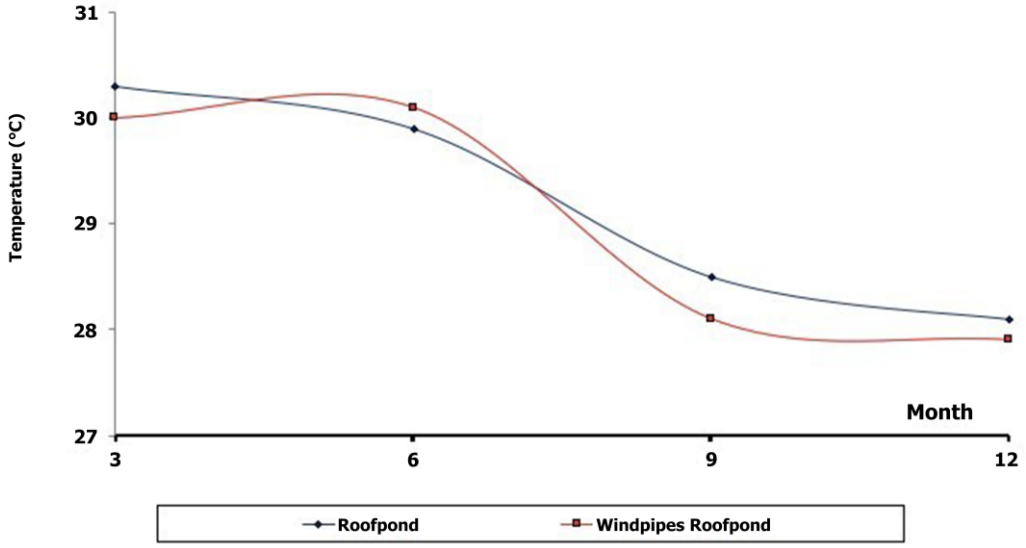

(a)

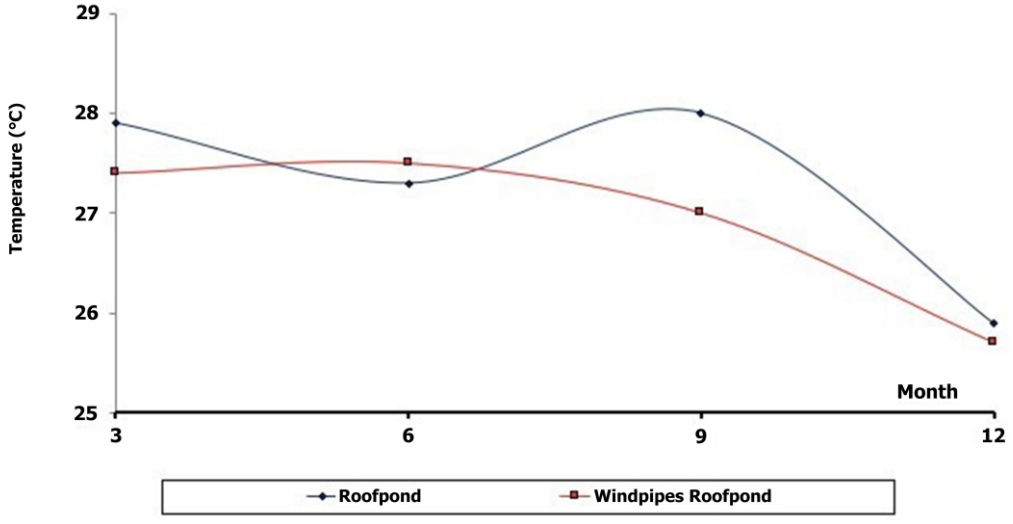

(b)

Figure 9. (a) Yearly Average Daytime Water Molecule Temperatures in 2021, (b) Yearly Average Night-time Water Molecule Temperatures in 2021

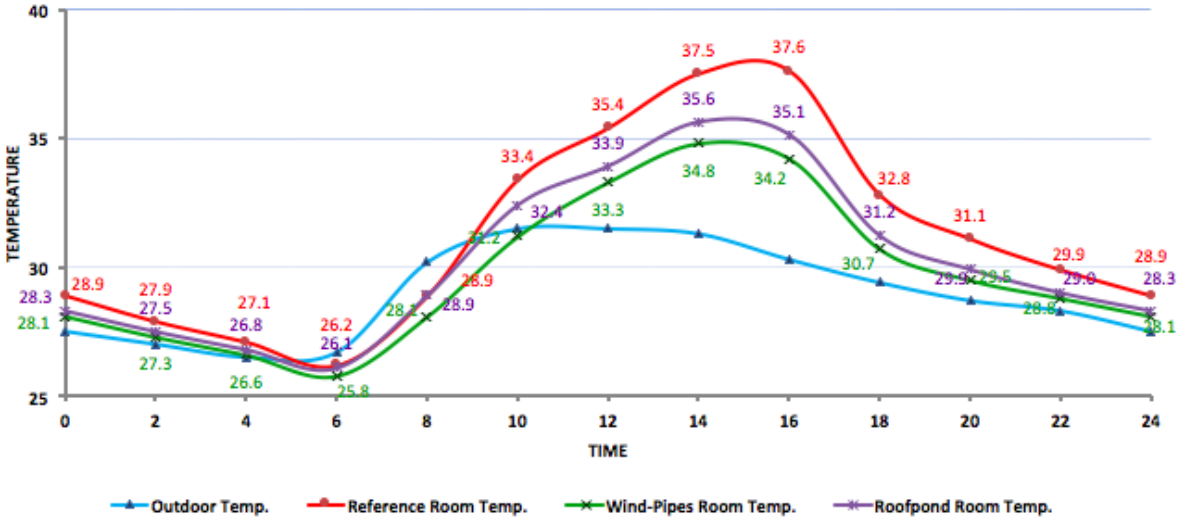
TEMPERATURE
TIME
Outdoor Temp.
Reference Room Temp.
Wind-Pipes Room Temp.
Roofpond Room Temp.

(a)

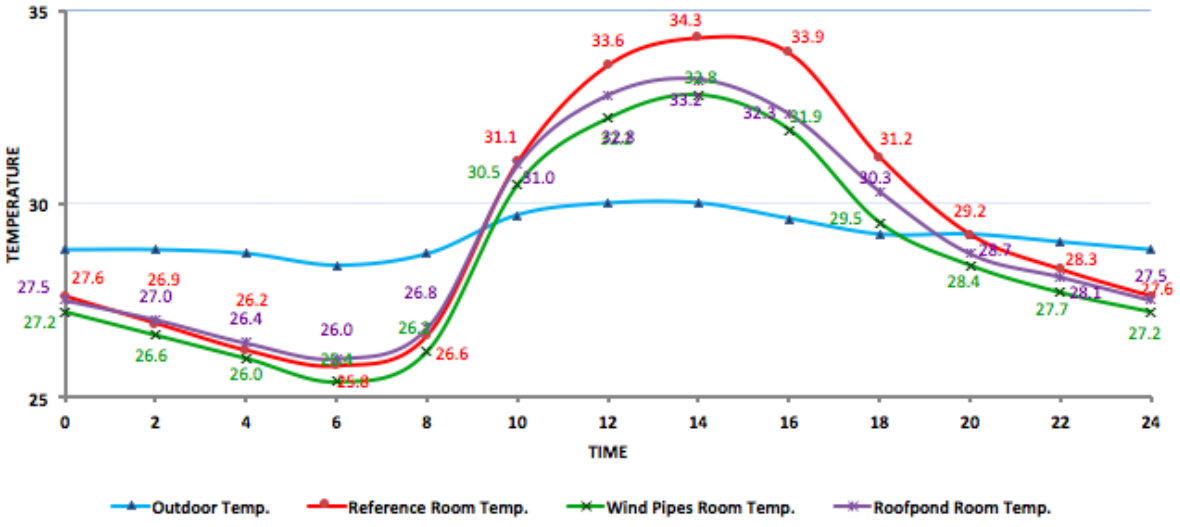
TEMPERATURE
TIME
Outdoor Temp.
Reference Room Temp.
Wind Pipes Room Temp.
Roofpond Room Temp.

(b)

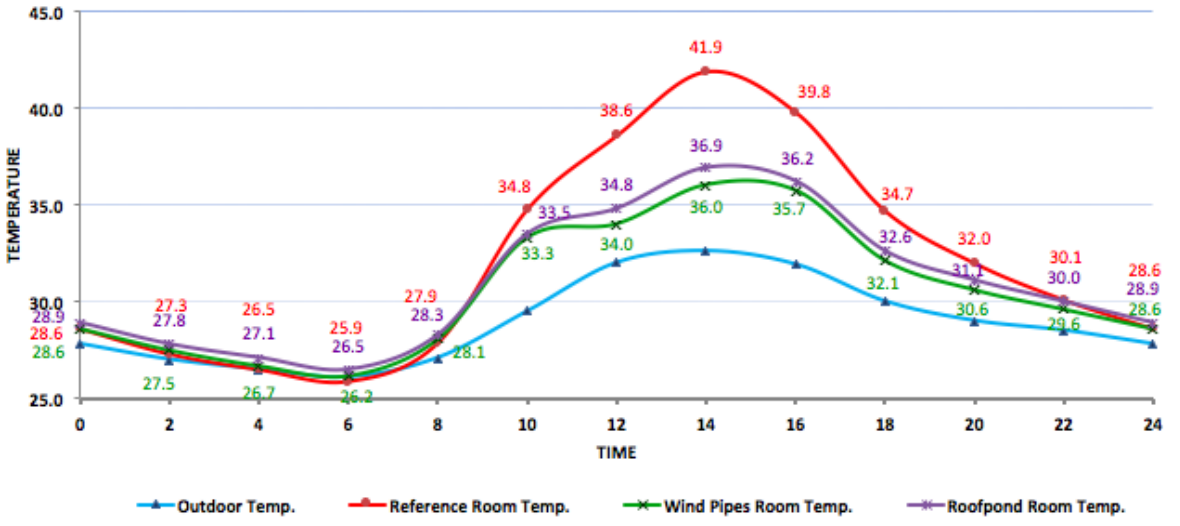
TEMPERATURE
TIME
Outdoor Temp.
Reference Room Temp.
Wind Pipes Room Temp.
Roofpond Room Temp.

(c)

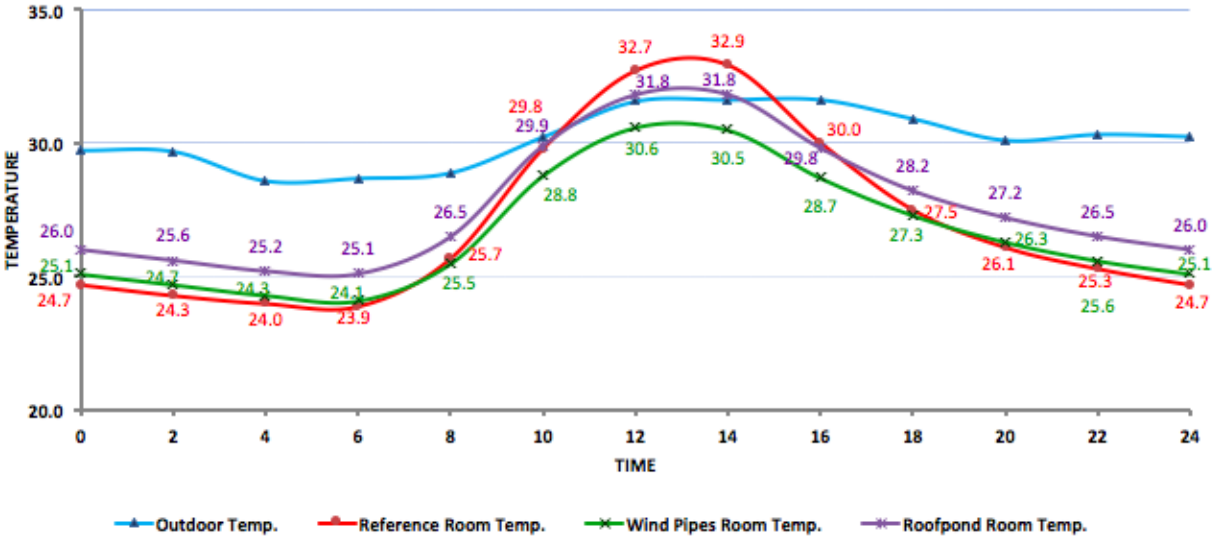

(d)

Figure 10. (a) Hourly Average Room Ambient Temperatures March 2021, (b) Hourly Average Room Ambient Temperatures June 2021, (c) Hourly Average Room Ambient Temperatures September 2021, (d) Hourly Average Room Ambient Temperatures December 2021.

Table 2. Yearly and hourly average min. & max. water & room ambient temperatures

WATER TEMPERATURE Month	Minimum Temperature (℃)	Maximum Temperature (℃)	Type of Roof	Cooling Loads (Watts) Day-Time
March	27.9	30.3	Conventional roof-pond	800
	27.4	30	Wind-driven tube roof-pond	1100
June	27.3	29.9	Conventional roof-pond	3000
	27.5	30.1	Wind-driven tube roof-pond	2400
September	28	28.5	Conventional roof-pond	5000
	27	28.1	Wind-driven tube roof-pond	5400
December	25.9	28.1	Conventional roof-pond	2900
	26.7	27.9	Wind-driven tube roof-pond	2400
ROOM TEMPERATURE	**Minimum Temperature (℃)**	**Maximum Temperature (℃)**	**Type of Roof**	**Nighttime**
March	27.3	31.1	Conventional roof-pond	600
	27.1	31.1	Wind-driven tube roof-pond	300
June	28.2	32.9	Conventional roof-pond	900
	27.9	32.5	Wind-driven tube roof-pond	400
September	28.7	33.5	Conventional roof-pond	700
	28.6	33.5	Wind-driven tube roof-pond	1600
December	27	31	Conventional roof-pond	1100
	26.7	30.3	Wind-driven tube roof-pond	0

Surprisingly, new models representing common flat concrete rooftops were added when testing room ambient temperatures, and their thermal performances were determined through comparison with the experimental models.

All the minimum room ambient temperatures during daytime obtained in March, June, September, and December were recorded at 6 am and not midnight while

all the maximum were recorded at 2 pm rather than noon as indicated in Figures10a, b, c, and, and their thermal details are presented in the following Table 2.

The daytime ambient room temperatures of wind-driven tubes rooftop recorded in June were found to be higher than the conventional roof-pond type by 0.4℃ due to the location of the sun at 23.5℃ degrees North latitude and the fact that the assessment was made during the dry season. However, the nighttime room temperatures were 0.3℃ lesser as indicated in Figure 11. For over a year, the wind-driven tubes roof-pond had a monthly average daytime room temperature of 27.2℃ which is better than the 27.4℃ recorded for the common type as presented in Table 2.

3.3.3. Saving Energy Roof Cooling Loads

According to ASHRAE (2021) [21], the fundamental approach to analyze the entire rooftop's heat gain is the resettlement method known as the CLTD (Cooling Load Temperature Difference).

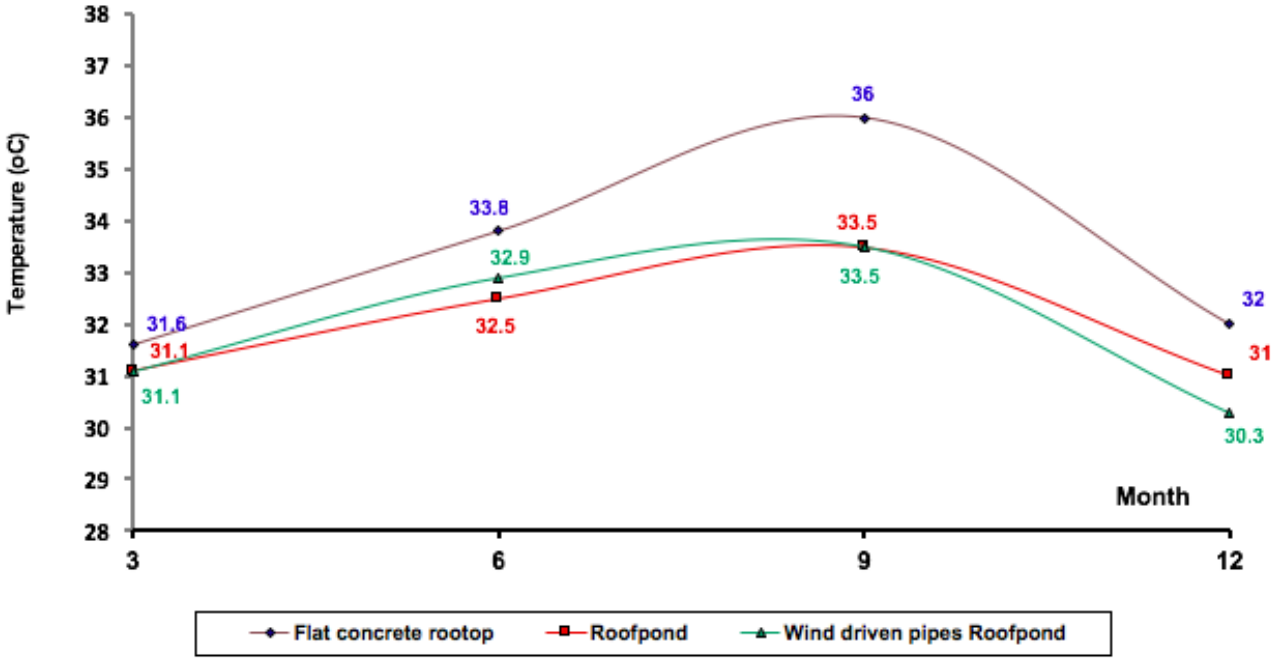

(a)

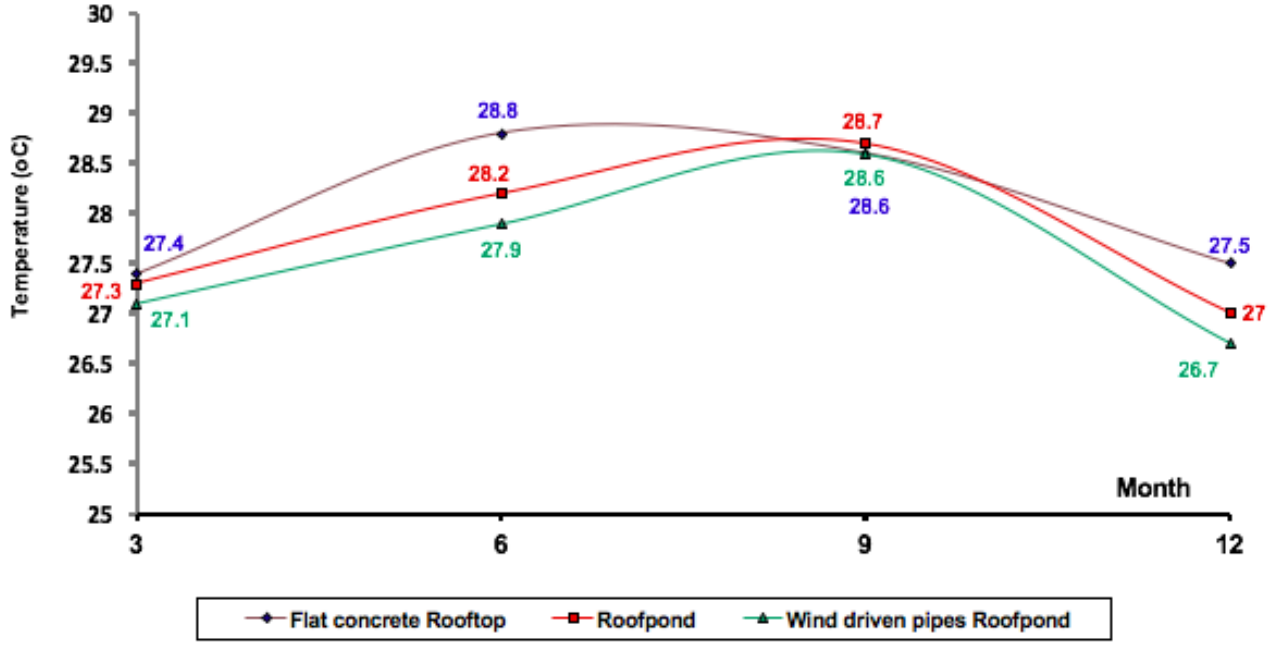

(b)

Figure 11. (a) Yearly Average Danytime Room Ambient Temperature in 2021. (b) Yearly Average Nighttime Room Ambient Temperature in 2021

Table 3. Annual daily average per-square meter cooling loads saved

NIGHTTIME:	**Cooling Loads 4 critical months (Watts/m^2)**	**Monthly average (Watts/m^2)**	**Daily average cooling loads (Watts/m^2)**
Wind-driven cutes roof-pond	2300	575	19
Conventional roof-pond	3300	825	27
COOLING LOADS SAVED:		**250 Watts/m^2**	
DAYTIME:			
Wind-driven cutes roof-pond	11300	2825	93
Conventional roof-pond	11700	2925	96
COOLING LOADS SAVED:		**100 Watts/m^2**	

The equation for the Energy Cooling load based on Mintorogo (2014) [22,23] is stated as follows:

$$q = UA\ x(CLTD)_{roof\text{-}pond} \quad (1)$$

Where:

q = Cooling Load
U = The overall heat transfer coefficient.
A = Area of rooftop
CLTD = Cooling Load roof-pond Temperature Difference ($T_o - T_1$)
T_o = Ambient room temperatures
T_1 = Water roof pond temperatures

Parameter setting:

U_{water} = approximately 1000 W/(m^2 °C). (TLV, 2022)[24]
$U_{concrete}$ = 2,985 W/(m^2 °C)
$A_{experimental\ model}$ = 1 m^2 (models = 1x1x1)

The monthly average cooling loads on the wind-driven iron tubes roof-pond during the daytime were observed to be lower compared to the conventional roof-pond by saving approximately 100 watts per square meter and more by night time with 250 watts per square meter as indicated in Table 3. This is due to the fact that the water temperatures on wind-driven tubes roof-pond during the nighttime are lower than the long-established water roof style presented in Table 2.

4. Conclusions

The simulation of the air movement in iron tubes and the mode of shading plates as well as the evaluation of the onsite experimental investigation led to the development of some assumptions to fill the research gap. Furthermore, the summary of the findings is stated as follows:

1) The installation of wind-driven tubes roof-pond toward the dominant direction, East and West, caused the wind to accelerate through the iron tubes. This proves that the convective wind blowing through all immersed tubes on the roof-pond and V-shading devices till 45 degrees can fasten the cooling water roof-pond and decrease cooling loads.
2) It was certified that when the veiling plate was directed 45 degrees toward the mild air, it tends to strengthen the convective cooling effect on the roof-pond.
3) The implementation of wind-driven tubes on a roof-pond caused the temperature of water elements to become cooler, relatively 0.5 to 1℃ during the night-time compared to the conventional type
4) The wind-driven tube roof-pond reduced the room ambient temperature slightly from 0.4 to 0.7℃ compared to ordinary and flat concrete roofs.
5) The cooling load's energy was saved at 100 to 250 Watts per square meter roof areas using wind-driven tubes roof-pond compared to the common type of roof-pond which is open-closed by day and night.
6) Saving energy operating mechanically layer roof-pond open and closed every day.

Acknowledgements

I would like to thank Sutrisno & Bagas Cahya Prabaswara for helping the CFD ANSYS results. I acknowledge Kuncoro for building tested model, and Wanda for editing the calculations.

REFERENCES

[1] Carrilho G. G., "Simulation of Wind-Driven Ventilative Cooling Systems for an Apartement Building in Beijing and Shanghai," Energy and Building, vol. 34, no. 1, pp. 1-22, 2002.

[2] Carrilho G. G., "Ventilative Cooling," M.Sc Thesis MIT, 1999.

[3] NASA, "Power Ceres Merra2 Native Resolution," 2022.

[4] India Buildtech. "Repair and Restoration of Multi-storied Buildings," 2022.

[5] Mintorogo D. S., "Predicting Thermal Performance of Roofing Systems in Surabaya," Dimensi Journal of Arch. and Built Environ, vol. 42, pp. 25–34, 2015.

[6] Roche P. La., Berardi U, "Comfort with Energy Savings with Active Green Roofs," Energy Build, vol. 82, pp. 492–504, 2014.

[7] Randdjelovic D. J., Vasov M., Ignjatovic M., Protic I. B., Kostic D., "Impact of Trombe Wall Construction on Thermal Comfort and Building Energy Consumption" Facta Universitatis, vol. 16, no. 2, pp. 279–292, 2018.

[8] Meteoblue, "Simulated Historical Climate and Weather Data for Surabaya," 2022.

[9] Weather Atlas, "Monthly Weather Forecast and Climate for Surabaya, Indonesia", 2022.

[10] Spanaki A., "Comparative Studies on Different Type of Roof ponds for Cooling Purposes: Literature Review," In Proceeding of 2nd PALENCIA and 28th AIVC Conference in Building Low Energy Cooling and Advanced Ventilation Technologies in 21th Century, Crete Island Greece, 2007.

[11] Spanaki A. et al., "On the Selection Design of the Proper Roof-pond Variant for Passive Cooling Purposes Review," Sustain Energy Rev., vol. 15, pp. 3523-33, 2011.

[12] Sharifi A., Yamagata Y., "Roof-pond as Passive Heating and Cooling Systems: A Systematic Review," Applied Energy, vol. 160, pp. 336-357, 2016.

[13] Sabir R., Muzaffar A., Hassan A., Nadeem AS., "Experimental Evaluation of Indirect Evaporative Cooler with Improved Heat and Mass Transfer," Applied Thermal Eng., vol. 217, pp. 119152, 2022.

[14] Givoni B., "Indoor Temperature Reduction by Passive Cooling Systems," Sol. Energy, vol. 85, pp. 1692-726, 2010.

[15] Spentzou E., Cook M. J., Emmitt S., "Low-Energy Cooling and Ventilation Refurbishments for Buildings in a Mediterranean Climate," Arch, Eng. and Design Management, vol. 18, no. 4, pp. 473-494, 2022.

[16] Ahmad A., Halil Z. A. B., "Hybrid Roof Pond System to Reduce Heat in Hot-Humid Climate for Buildings," URRCME, vol. 6, issue 2 pp. 15-25, 2019.

[17] Kharrufa S. N., Adil Y., "Upgrading the Building Envelope to Reduce Cooling Loads," Energy Build, vol. 55, pp. 389-96, 2012.

[18] Voster J., Dobson. R., "Sustainable Cooling Alternatives for Buildings," J Energy Southern Africa, vol. 22, pp. 48-66.

[19] Sodha M., Singh S., Kumar A., "Thermal Performance of a Cool-pool System for Passive Cooling of a non-conditioned Building," Build. Environ, 1985, vol. 20, pp. 233-40, 1985.

[20] Mintorogo D. S., Widigdo W. K, Juniwati A. "A Pumice Layer: Solution to Diminish Thermal on Horizontal Leftover Rooftop Places," Dimensi: Journal of Architecture and Built Environment, vol. 46, pp. 155–159, 2019.

[21] ASHRAE. "ASHRAE Handbook Fundamentals," I-P Edition, Supported by ASHRAE Research. Atlanta, G. A. American Society of Heating, Refrigerating and Air-Conditioning Engineering USA. 2021

[22] Mintorogo D. S., "Application of Pakis Stem as Insulation to Control Heat Gain on Concrete Flat Roof," Dissertation, Doctor of Philosophy-Universiti Teknologi Malaysia, Johor-Bahru, Malaysia, 2014.

[23] Khakre V. V., Wankhade A., Ali M. A., "Cooling Load Estimation by CLTD Method and Hap 4.5 for an Evaporative Cooling System," IRJET, vol. 4, issue 1, pp. 1457-1460, 2017.

[24] TLV, A Steam Specialist Company, 2022.